

The Role of Drifts in the Plasma Transport at the Tokamak Core-SOL Interface

A.V. Chankin* and D.P. Coster

Max-Planck-Institut für Plasmaphysik, EURATOM Association, 85748 Garching, Germany

Abstract

The interface between the core (inside the magnetic separatrix in X-point configurations) and the scrape-off layer (SOL) of tokamaks is a delicate region of the magnetic topology transition from closed to open field lines where neither the standard neoclassical theory nor the SOL physics fully apply. Sharp gradients of plasma parameters in the outer core, caused by the proximity of divertor sinks in the near SOL, invalidate some ordering assumptions of the neoclassical theory. At the same time, the existence of closed flux surfaces in the core enforces ambipolarity of radial plasma flows, in difference to the situation in the SOL where the current loop may close through the divertor. Detailed analysis of the plasma transport and flows with the emphasis on the outer core region, just inside the separatrix, is carried out in the paper, based on EDGE2D modelling and analytical formulas.

JNM keywords: Plasma-Materials Interaction, Plasma Properties

PSI-20 keywords: JET, EDGE2D, drifts, SOL transport

PACS: 52.55.Fa, 52.40.Hf, 52.65.-y, 52.25.Fi

**Corresponding author address:* Max-Planck-Institut für Plasmaphysik, Boltzmannstr. 2,
85748 Garching, Germany

**Corresponding author E-mail:* Alex.Chankin@ipp.mpg.de

Presenting author: Dr A.V. Chankin

Presenting author E-mail: Alex.Chankin@ipp.mpg.de

1. Introduction

This work was inspired by a pioneering work of Goldston [1] predicting the power width at the divertor target (Eqs. (5,6) of [1]) and particle confinement time τ_p (Eq. (3)) for low-gas-puff, low density H-mode tokamaks. It is based on the assumption that the SOL density width is determined by the penetration length of ions through the separatrix by ion ∇B and centrifugal ($\nabla B + \text{cent.}$) drifts in the absence of strong anomalous particle transport. It also requires a rather low recycling rates which otherwise would influence the SOL density width. Further, the model assumes that the anomalous perpendicular electron heat conduction coefficient χ_e is greater than the effective diffusion coefficient associated with the ion drift transport, $\chi_e > D_{i,eff}$, the condition likely to be fulfilled due to smallness of $D_{i,eff}$. The ion transport thus sets the SOL density width which can be easily ‘filled’ by electron energy regardless of the particular electron heat transport mechanism. The drift-based model of [1] was shown to be in a good agreement with experimental scalings for the power width. In addition, the model was also used to estimate the maximum ion current that can be carried by $\nabla B + \text{cent.}$ drifts, $I_{loss} \sim 4\pi an_{sep} T_{sep} / B$, and the associated particle confinement time τ_p . This estimate requires a factor 2 ion pressure up-down asymmetry, which is possible provided there are some other non-ambipolar mechanisms apart from drifts, e.g. a stochastic layer around the separatrix. Cross-field drifts containing a radial component relevant to the present study are shown in Fig. 1. With $E \times B$ drifts being intrinsically ambipolar, electric charge can be carried across the flux surface only by $\nabla B + \text{cent.}$ drifts, with the vertical guiding centre (g.c.) current density flux given (approximately, see below) by $2(p_e + p_i) / eBR$. The total charge outflow from the bottom half of the torus must be equal to the

inflow from the top half, to satisfy quasineutrality. Hence, $(p_e + p_i)$ must be up-down symmetric, in the absence of other non-ambipolar mechanisms. The above estimate for I_{loss} , if confirmed, would therefore indicate the presence of some other non-ambipolar mechanisms apart from drifts (Sec. 5). At the same time, the main result of [1]: the estimate of the SOL power width, is unaffected by possible other non-ambipolar mechanisms, as long as they influence mostly electrons but not the ions.

2. EDGE2D modelling

EDGE2D cases with drifts suffer from poor stability, which is influenced by the presence of impurities, details of the magnetic configuration, boundary parameters, grid resolution and some other factors. For this study, a low density pure deuterium EDGE2D case with drifts was run, with separatrix electron density $n_{e,sep} = 0.6 \times 10^{19} \text{ m}^{-3}$, controlled by gas puff and recycling (see the setup of EDGE2D runs in [2]), with 3 MW of input power in the ion and 2 MW in electron channels, with $I_p/B_t = 2 \text{ MA}/2 \text{ T}$, spatially constant radial transport coefficients $D_{\perp} = 0.5 \text{ m}^2$ and $\chi_{e,i} = 1.5 \text{ m}^2$, and with the configuration of JET #56723 (see Fig.2, also [2]), with 16 poloidal rings in the core and SOL. The ion ∇B drift was down. For such a low $n_{e,sep}$, temperatures $T_{e,i}$ were almost constant on core flux surfaces, as intended, since poloidally constant temperatures greatly facilitate analysis of the code output. However, separatrix collisionalities were too low: $\nu_{ii}^* = 0.4$, with ions being in the Plateau regime, and $\nu_{ei}^* = 1.35$ - with marginally collisional electrons. Hence, the results of this study may only be qualitative and indicative of some important physics mechanisms.

3. Up-down asymmetries and radial plasma flows

Outer midplane (OMP) profiles are shown in Fig. 3. At the separatrix, ion poloidal Larmor radius, $\rho_{i\theta} = 1$ cm, is close to the decay length of the ion pressure, $\lambda_{p_i} = 1.2$ cm, the situation often encountered in H-modes. Such a sharp ion pressure profile invalidates an assumption of the standard neoclassical theory which requires $\rho_{i\theta} \ll \lambda$ (see. e.g. [3]), with λ being the decay length of plasma parameters. This greatly increases ion parallel viscosity $\Pi_{i\parallel}$, plotted in Fig. 4 together with ion static pressure along the outermost core ring c01. In EDGE2D, poloidal distance is counted from the outer to the inner target.

The ion static pressure shows a significant in-out (high field side – low field side) asymmetry, which will be discussed later in Sec. 5 together with ion parallel flows that determine $\Pi_{i\parallel}$. At the same time, the pressure up-down asymmetry is small. The latter is a necessary condition for zeroing the net drift-related charge flow across the separatrix, as pointed out in the Introduction. Indeed, in the core, in the absence of other non-ambipolar mechanisms, radial drift flows of ions and electrons must be equal. For electrons, smallness of their net radial flow follows from their near Boltzmann distribution: $n_e \sim \exp(e\Phi/T_e)$, resulting (for $T_e(\theta) = \text{const}$) in the cancellation between their radial diamagnetic flux $cT_e \partial n_e / \partial l_\theta / eB \sim -cn_e E_\theta / B$ and radial E×B flux $cn_e E_\theta / B$ locally, at each poloidal position regardless of the shape of the $n_e(\theta)$ profile. For ions, however, diamagnetic and E×B flows due to up-down pressure asymmetry add to each other, hence, p_i must be fairly up-down symmetric to ensure the ambipolarity of the plasma flow, with the $p_i(\theta)$ up-down symmetry being achieved by the adjustment of the radial electric field E_r

driving compressible poloidal E×B flow. A similar cancellation for electrons can be also obtained using g.c. drifts, by writing electron fluxes as $\Gamma_{\nabla B+cent.} = 2cp/eBR \times \partial R/\partial s_\theta$, $\Gamma_{E \times B} = -cn/B \times \partial \Phi/\partial s_\theta$, combining the two drifts into $\Gamma_{drift} = cT/eBR^2 \times \partial(nR^2)/\partial s_\theta$, and

calculating the total flow across the flux surface: $\Gamma_{total} = \int_{s_\theta=0}^{2\pi} \Gamma_{drift} ds_\theta \times 2\pi R =$

$$\int_{s_\theta=0}^{2\pi} 2\pi cT/eBR \times \partial(nR^2)/\partial s_\theta = 0 \text{ due to } BR = const(\theta). \text{ Hence, the near cancellation of the radial}$$

electron flow, to the degree T_e is poloidally constant and n_e is distributed according to the Boltzmann law, follows from the cancellation between integral $\nabla B+cent.$ and E×B flows. In particular, any up-down density asymmetry, leading to the net ion flow due to $\nabla B+cent.$ drifts, will be cancelled by the E×B flow in the R direction arising from vertical electric field (E-field).

In the strictest formulation in flux coordinates, surface-averaged flux of species j can be obtained from the momentum balance equation (Eq. (2.15) of [3]), giving:

$$\langle n_j \mathbf{u}_j \cdot \bar{\nabla} \Psi \rangle = -c/e_j \langle R^2 \bar{\nabla} \xi \cdot (e_j n_j \mathbf{E} + \mathbf{F}_j) \rangle + c/e_j \langle R^2 \bar{\nabla} \xi \cdot \bar{\nabla} \bar{P}_j \rangle + c/e_j \partial/\partial t \langle n_j m_j R^2 \bar{\nabla} \xi \cdot \mathbf{u}_j \rangle, \quad (1)$$

where the notations are standard, with ψ being poloidal flux, $\bar{\nabla} \xi$ - unit vector in the toroidal direction divided by major radius R , \bar{P}_j - pressure-stress tensor, \mathbf{F}_j - friction force, and $\langle \dots \rangle$ denoting flux surface averaging defined by Eqs. (2.55-2.67) of [3]. For electrons, neglecting their small viscosity and classical diffusive flux caused by perpendicular friction force with ions, and for steady state conditions, one obtains the neoclassical flux: $\langle n_e \mathbf{u}_{e,nc} \cdot \bar{\nabla} \Psi \rangle =$

$-c \langle R^2 \bar{\nabla} \xi \cdot (en_e \mathbf{E} + \mathbf{F}_{e,\parallel}) \rangle / e$ (Eq. (2.95) of [3]). Neglecting also the (usually small) Ware pinch

related to the toroidal E-field (the only component present in this equation, since $\vec{\nabla} \xi \cdot \mathbf{E}_\perp = 0$), one arrives at a conclusion that the net radial electron flow is determined by the surface-averaged electron-ion friction force. This friction force arises due to the Pfirsch-Schlüter (P-S) current, and contributes to the poloidal E-field and associated $\mathbf{E} \times \mathbf{B}$ drift in the R-direction as shown in Fig. 1, giving the P-S diffusion. In the circular geometry with concentric flux surfaces and $r/R \ll 1$, the P-S diffusion coefficient is given by $D_{P-S} = 1.2q^2(T_e + T_i)v_{ei}/(m_e\omega_e^2)$ (Eq. (4.102) of [3], with k-coefficients in Table II on p. 267)). The ratio of the P-S flow ($D_{P-S}dn/dr \times 2\pi a 2\pi R$) to the particle flow associated with $I_{loss} \sim 4\pi an_{sep}T_{sep}/B$, is $1.2\pi q^2(1+T_e/T_i)v_{ei}/\omega_e \times R/\lambda_n$, where λ_n - density decay length. For JET parameters at the separatrix with $R=1.5$ m, $\lambda_n = 1$ cm, safety factor $q=3$, $T_e=T_i$, $n_e=1 \times 10^{19}$ m⁻³, $T_e=100$ eV, $B=3$ T, this ratio is equal to 1/80. Hence, the typical drift flow through the separatrix must be by 2 orders of magnitude lower than the value calculated from the ∇B +cent. drifts by assuming factor 2 up-down pressure asymmetry.

Owing to the large role played by parallel ion viscosity, a certain degree of up-down asymmetry in the ion static pressure on closed field lines is nevertheless possible. The quantity that has to exhibit the complete up-down symmetry should be related to the vertical guiding centre (g.c.) non-ambipolar drifts (∇B +cent. drifts) for both ions and electrons. After simple transformations, to account for larger ion centrifugal drift velocity compared to the ∇B drift velocity (for the same kinetic energy), and neglecting electron viscosity, one arrives at the (newly introduced) ‘current pressure’: $p_{current} = p_{i,static} + \Pi_{i\parallel}/4 + n_i m_i v_{i\parallel}^2/2 + p_e$. Here $\Pi_{i\parallel}$ - parallel ion viscosity excluding ‘dynamic pressure’ $n_i m_i v_{i\parallel}^2$. Fig. 5 shows poloidal profiles of the ‘current pressure’ for the 1st

ring (c01) inside the separatrix, together with rings 4, 7 and 10 further inward, and for the 1st ring outside of the separatrix in the SOL and divertor (s01), together with rings 4, 7 and 10 further outward. The current pressure profiles look qualitatively similar to those of the ion static pressure or total static pressure ($p_e + p_i$) ones due to the presence of the coefficient $\frac{1}{4}$ before viscosity and a relatively small contribution from dynamic pressure $n_i m_i v_{i\parallel}^2$ (except for positions close to the target in the divertor, where the Mach number is high). In the core, all profiles are up-down symmetric, while in the SOL a clear up-down asymmetry in favour of the bottom half of the torus is seen, as expected from the effect of the ion $\nabla B + \text{cent.}$ drifts. Radial transport in the SOL is, generally, non-ambipolar, with the current loop closing through the divertor.

4. Plasma flows and in-out asymmetries at the core edge

An interesting feature of core current pressure profiles shown in Fig. 5, which is also seen on n_e profiles, is a significant in-out asymmetry in favour of the inner (high field) side, with the surface variable part being $\sim 1/3$ of the surface average value, which is explained later in this section. Owing to a nearly Boltzmann distribution of electrons, this also implies a large in-out asymmetry in the electric potential Φ . Fig. 6 shows poloidal profiles of Φ and the Mach number of the parallel ion flow on the 1st ring inside the separatrix. The Φ in-out asymmetry implies a significant outward (along R) E-field generating downward $E \times B$ drift shown schematically in Fig. 1. In the SOL, ion $\nabla B + \text{cent.}$ drifts down together with the poloidal $E \times B$ flow pump particles to the lower half of the torus, with the particle flow loop being closed by ion flows along field lines from bottom to top ('ion Pfirsch-Schlüter flows', see e.g. [4]). In Fig. 6, the same $\sin(\theta)$ -shaped feature of the Mach number profile as in the SOL is seen, with surface variable ion parallel flows from top to bottom. Its origin is however different. It is entirely attributed to the

large downward $E \times B$ drift, while the combination of the ion $\nabla B + \text{cent.}$ drifts and poloidal $E \times B$ flow would contribute to the (smaller) parallel flow in the opposite direction (from top to bottom). This is due to the opposite signs of radial electric field E_r in the core and in the SOL (so that the two contributions are added in the SOL but subtracted in the core) and the fact that the influence of the $E \times B$ flow outweighs that from the ion $\nabla B + \text{cent.}$ drifts (or, using the fluid formulation, outweighs the influence of the ion diamagnetic flow). The large negative E_r extracted from EDGE2D for the 1st ring inside the separatrix can be expressed through gradients of plasma parameters by using a numerical coefficient (a fitting parameter) before the ion temperature gradient as follows: $eE_r = \nabla p_i / n_e + 1.29 \nabla T_i$. Since this coefficient is positive, the poloidal $E \times B$ flow is numerically larger than the ion diamagnetic flow and should therefore drive the P-S flow in the opposite direction to that seen in the SOL. But, due to the presence of large vertical $E \times B$ flow, as pointed out above, the parallel ion flow profile looks qualitatively similar to that seen in the SOL. The coefficient 1.29 lies in between the values 0.5 and 2.1 obtained for Plateau and P-S regimes, respectively, derived for the simplest circular configuration with concentric flux surfaces and $r/R \ll 1$, as follows from [6] for the expression for poloidal velocity (see Eqs. (68-69), and we neglect the effect of a small toroidal momentum; also note that the coefficient before ∇T_i here corresponds to $-k$ in [6]). This coefficient therefore is not inconsistent with the neoclassical theory for a near separatrix plasma of the analyzed EDGE2D case, which is on the border between the Pfirsch-Schlüter and Plateau regimes.

The surface-averaged parallel ion flow shown in Fig. 6 is in the co-current direction. This should be attributed to the perpendicular viscosity (2nd term on the right hand side (RHS) of Eq. (1)) due to the presence of the co-current plasma rotation in the SOL (where such a flow is

experimentally observed and calculated in the codes, see e.g. [5]). The mechanism of radial transport of poloidal velocity from the SOL to the core was discussed in [6,7].

The origin of the large ion-out density asymmetry is attributed to the mechanism of a compressible poloidal plasma E×B flow which scales as $E_r / B \times 2\pi R \propto R^2$. Under an extreme (and unphysical) assumption of a finite E_r but $T_i \rightarrow 0$, this would lead to a factor 4 in-out density asymmetry for a machine with $r/R = 1/3$. In reality, T_i and E_r are related to each other, and pressure tends to reach the equilibrium along field lines. The $\rho_{i\theta} \approx \lambda_{p_i}$ equality in this EDGE2D case achieved at the separatrix implies that poloidal E×B drift velocity $cE_r / B \sim c\nabla p_i / enB \sim cT_i / e\lambda_{p_i} B$ is close to the poloidal projection of ion thermal velocity $\sqrt{T_i / m_i} \times B_\theta / B$. The poloidal E×B drift under such conditions can strongly perturb the pressure distribution over the flux surface via the transfer of parallel momentum in the diamagnetic direction, leading to a substantial ion-out pressure asymmetry in favour of the inner (high field) side.

5. Possible influence of field line stochastization on plasma flows

As pointed out earlier, arguments against the build up of large up-down pressure asymmetries, leading to the estimate $I_{loss} \sim 4\pi an_{sep} T_{sep} / B$ for the ion current crossing the separatrix, should be waved provided there is an additional non-ambipolar mechanism in this region such as field line stochastization. If electrons are allowed to escape through the separatrix by following stochastic field lines, then E_r in the core becomes more positive compared to prescriptions of the neoclassical theory while ions can follow electrons via an entirely neoclassical mechanism. More

positive, or less negative, E_r leads to the build-up of up-down pressure asymmetries and the net large radial flow of ions (but not electrons!) due to ∇B +cent. drifts. The deviation from the neoclassical E_r can be measured in the experiment. Further, radial ion flow creates the $j \times B$ force accelerating the plasma toroidally in the co-current direction (with no such force for electrons following stochastic field lines). The generation of toroidal momentum is described by equating the LHS of Eq. (1) to the last term on its RHS, with a possible contribution from viscosity, 2nd term on the RHS (see also Eq. (6.58) of [3], where it is considered for transient processes, since neoclassical transport on long time scales is ambipolar). In the presence of stochastization the $j \times B$ force exerts a permanent toroidal torque on the plasma (see e.g. [9,10]). The resulting toroidal momentum is a measurable quantity (but requires measurements at different poloidal locations).

6. Summary

Poloidal distributions of plasma parameters around the separatrix position under the conditions of high temperatures and sharp radial gradients of density and temperatures were modelled with the 2D fluid code EDGE2D. Large in-out (high field side – low field side), but small up-down asymmetries of plasma density, pressure and electric potential just inside of the separatrix, follow from the code, in contrast with one of the assumptions of the heuristic model [1] which required a factor two up-down pressure asymmetry for the prediction of the ion loss current through the separatrix and the τ_p estimate. Such an assumption can only be made if one assumes the presence of other non-ambipolar processes of radial plasma transport in addition to drifts, e.g. anomalous radial electron transport caused by stochastization of magnetic field lines. The contribution of such processes to the radial transport could be experimentally detected via

measurements of radial electric field and toroidal momentum inside the separatrix, in addition to direct experimental validation of τ_p estimates of [1] and possibly, up-down pressure asymmetries along the separatrix flux surface. Further EDGE2D modeling of the near separatrix region is envisaged, by running cases with increased density (and hence, collisionality), to cover the range of separatrix collisionalities encountered in experimental conditions.

Acknowledgement

Stimulating discussions with Prof. P.C.Stangeby and members of the JET TFE2 edge modeling group are acknowledged.

References

- [1] R.J.Goldston, Nucl. Fusion **52** (2012) 013009.
- [2] A.V.Chankin, D.P.Coster, G.Corrigan et al., Plasma Phys. Control. Fusion **51** (2009) 065022.
- [3] F.L.Hinton and R.D.Hazeltine, Rev. Mod. Phys. **48** (1976) 239.
- [4] N.Asakura, S.Sakurai, M.Shimada et al., Phys. Rev. Lett. **84** (2000) 3093.
- [5] A.V.Chankin, J. Nucl. Mater. **241-243** (1997) 199.
- [6] R.D.Hazeltine, Phys. Fluids **17** (1974) 961.
- [7] V. Rozhansky, Plasma Phys. Control. Fusion **46** (2004) A1–A17
- [8] P A Molchanov, V A Rozhansky, S P Voskoboynikov, et al., Plasma Phys. Control. Fusion **50** (2008) 115010
- [9] A.V.Chankin and W.Kerner, Nucl. Fusion **36** (1996) 563.
- [10] E.Kaveeva, V.Rozhansky and M.Tendler, Nucl. Fusion **48** (2008) 075003.

Figure captions

Fig. 1. Drifts with the radial component, near the separatrix. Vertical $E \times B$ drift is discussed in

Sec. 4.

Fig. 2. Magnetic equilibrium

Fig. 3. Outer midplane (OMP) profiles

Fig. 4. Poloidal profiles at 1st ring inside separatrix

Fig. 5. 'Current pressure' profiles.

Fig. 6. Profiles along 1st ring inside separatrix.

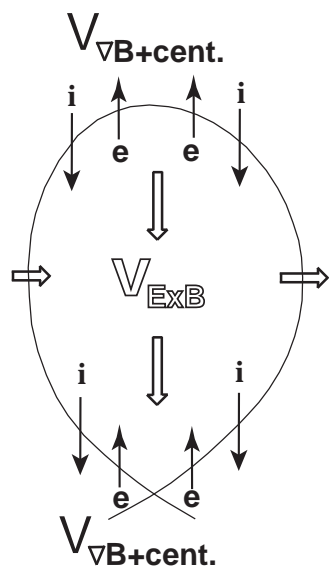


Fig. 1



Fig. 2

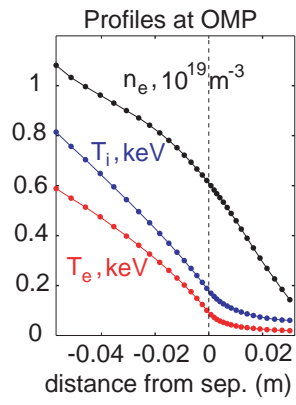


Fig. 3

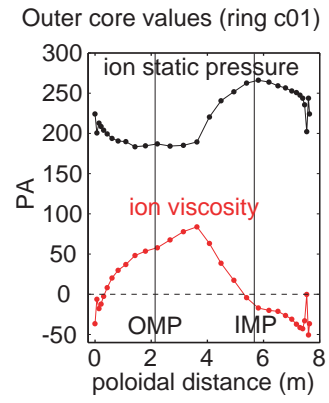


Fig. 4

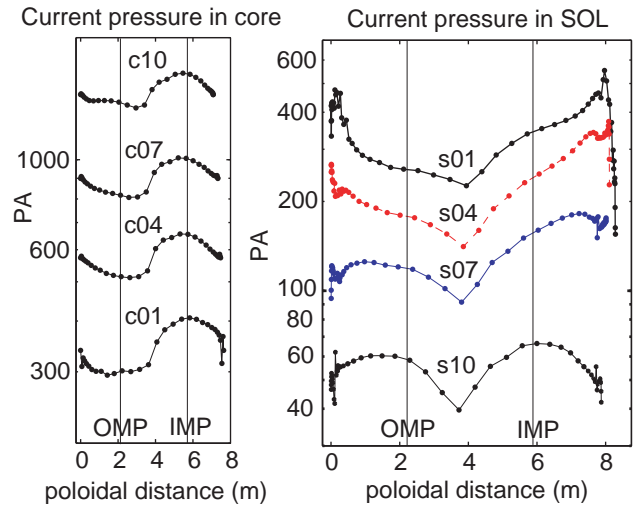


Fig. 5

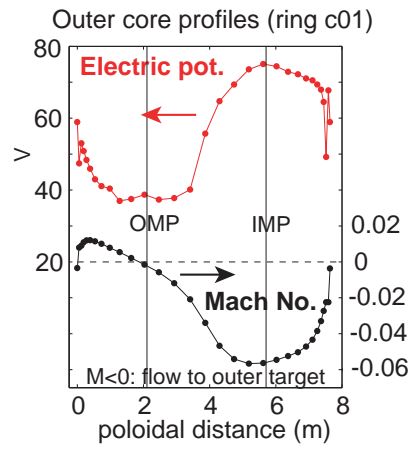


Fig. 6